Dark-Matter Decay as a Complementary Probe of Multicomponent Dark Sectors

Keith R. Dienes,[1,2] Jason Kumar,[3] Brooks Thomas,[4] and David Yaylali[3]

[1]*Department of Physics, University of Arizona, Tucson, Arizona 85721 USA*
[2]*Department of Physics, University of Maryland, College Park, Maryland 20742 USA*
[3]*Department of Physics, University of Hawaii, Honolulu, Hawaii 96822 USA*
[4]*Department of Physics, Carleton University, Ottawa, Ontario K1S 5B6 Canada*

In single-component theories of dark matter, the $2 \to 2$ amplitudes for dark-matter production, annihilation, and scattering can be related to each other through various crossing symmetries. The detection techniques based on these processes are thus complementary. However, *multicomponent* theories exhibit an additional direction for dark-matter complementarity: the possibility of dark-matter *decay* from heavier to lighter components. We discuss how this new detection channel may be correlated with the others, and demonstrate that the enhanced complementarity which emerges can be an important ingredient in probing and constraining the parameter spaces of such models.

Introduction.—In recent years, many search techniques have been exploited in the hunt for dark matter. These include possible dark-matter production at colliders, dark-matter scattering at underground experiments, and indirect detection through dark-matter annihilation at terrestrial or satellite-based experiments. However, the three dark-matter processes which underlie these different search techniques are related to each other through crossing symmetries, and thus depend on a single underlying interaction which couples dark matter to ordinary matter. This is the origin of the celebrated complementarity which connects the different existing dark-matter search techniques. For a review, see Ref. [1].

As sketched in Fig. 1(a), most complementarity studies implicitly assume a single dark-sector particle χ. In this Letter, by contrast, we point out that this situation becomes far richer in *multicomponent* theories of dark matter. In particular, if the dark sector consists of at least two different dark-matter components χ_i and χ_j with differing masses $m_i \neq m_j$, then for $i \neq j$ dark-matter production becomes *asymmetric* rather than symmetric; dark-matter annihilation of one dark particle against itself or its antiparticle becomes *co-annihilation* between two different dark species; and dark-matter scattering—previously exclusively elastic—now becomes *inelastic*, taking the form of either "up-scattering" [2] or "down-scattering" [3]. Moreover, even more importantly, an entirely new direction for dark-matter complementarity opens up: this is the possibility of dark-matter *decay* from heavier to lighter dark-matter components. This process corresponds to the *diagonal* direction in Fig. 1(b), and thus represents an entirely new direction for dark-matter complementarity. Of course, we are not the first to discuss decaying dark matter of this form (see, *e.g.*, Refs. [3–5] for prior work). However our main point is that these decays are actually part of a larger complementarity,

and that this enhanced complementarity can be an important ingredient in probing and constraining the parameter spaces of theories with nontrivial dark sectors.

Two examples.—As illustration of how this works, we consider a dark sector with two Dirac fermions χ_1 and χ_2 which are neutral under all Standard-Model gauge symmetries and have masses m_1 and m_2 respectively, with $m_2 > m_1$. The fundamental four-point dark-matter–quark interaction in Fig. 1(b) is given by a flavor-conserving effective four-Fermi contact operator. For concreteness, we shall consider two operators, the scalar (S) and the axial-vector (A) interactions

$$\mathcal{L}_{\text{int}}^{(S)} = \sum_{q=u,d,s,\dots} \frac{c_q^{(S)}}{\Lambda^2} (\bar{\chi}_2 \chi_1)(\bar{q}q) + \text{H.c.},$$

$$\mathcal{L}_{\text{int}}^{(A)} = \sum_{q=u,d,s,\dots} \frac{c_q^{(A)}}{\Lambda^2} (\bar{\chi}_2 \gamma_\mu \gamma^5 \chi_1)(\bar{q}\gamma^\mu \gamma^5 q) + \text{H.c.} \quad (1)$$

These operators give rise to spin-independent (SI) and spin-dependent (SD) scattering, respectively. Here q denotes the quark flavor, c_q the dark-matter–quark coupling, and Λ the mass scale of the new physics.

Note that even though we have restricted our attention to operators such as those in Eq. (1) which only couple χ_i to χ_j with $i \neq j$, a more general theory involving four-Fermi operators of this sort is likely to include the "diagonal" $i = j$ operators as well. However, such "diagonal" operators appear even in single-component theories of dark matter and thus do not represent the new physics we wish to explore in this Letter. We shall therefore restrict our attention to $i \neq j$ here. It would nevertheless be of interest to study the experimental complementarity bounds that emerge when all of these operators are included simultaneously [6].
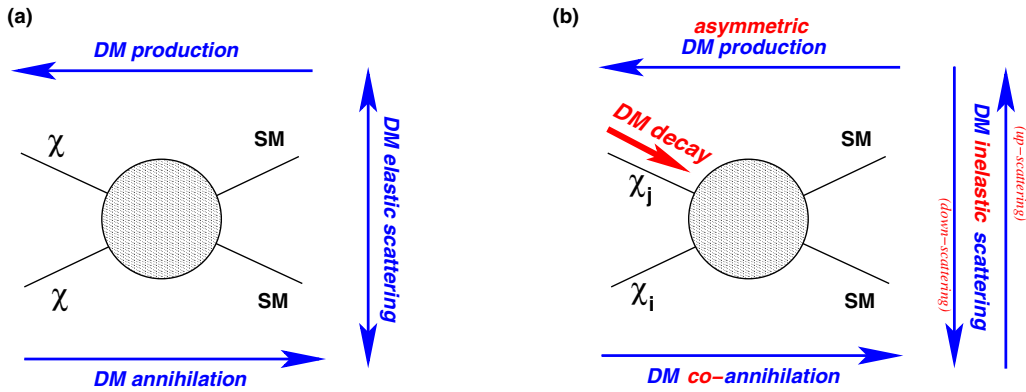
FIG. 1 (color online). (a) In single-component theories of dark matter, the $2 \to 2$ amplitudes for dark-matter production, annihilation, and scattering correspond to different directions (blue arrows) for the imagined flow of time through a single four-point diagram. (b) In *multicomponent* theories of dark matter, by contrast, dark-matter production becomes *asymmetric* rather than symmetric; dark-matter annihilation of one dark species with itself becomes *co-annihilation* between two different dark species; and elastic dark-matter scattering becomes *inelastic*. Even more importantly, however, the existence of a nonminimal dark sector opens up an additional process: dark-matter *decay* from heavier to lighter dark-matter components. This process corresponds to a *diagonal* direction for the imagined flow of time, as shown, and thus represents a new direction for dark-matter complementarity.

Note that since the operators in Eq. (1) are nonrenormalizable, they can only be interpreted within the context of an effective field theory whose cutoff scale is parametrically connected to Λ. As a result, our use of such operators implicitly presupposes that the energy scales of the processes we shall consider do not exceed Λ. Assuming $\mathcal{O}(1)$ operator coefficients, this requires $\Lambda \gtrsim \mathcal{O}(\text{GeV})$ for direct-detection bounds; for dark-matter annihilation this requires $\Lambda \gtrsim \mathcal{O}(m_1, m_2)$; and for dark-matter decays of the form $\chi_2 \to \chi_1 \bar{q} q$ this requires $\Lambda \gtrsim \mathcal{O}(\Delta m_{12})$. For collider-production bounds, the use of such operators is strictly valid only if $\Lambda \gtrsim \mathcal{O}(\text{TeV})$. If this last condition is not met, the resulting collider bounds should be viewed only as heuristic, and one would require a more complete theory (for example, involving potentially light mediators connecting the dark and visible sectors) before being able to make more precise statements. We also remark in this context that the scalar operator structure explicitly violates the chiral symmetries of the Standard Model. The coefficient of this operator thus implicitly includes a factor of the vacuum expectation value of the Higgs field, so that we would in this case more precisely identify $\Lambda' \equiv (\Lambda^2 v)^{1/3}$ as the scale of new physics. Our previous constraints for Λ then apply to Λ'.

We now make two further assumptions. First, we assume

$$c_u = -c_d = c_c = -c_s = c_t = -c_b \equiv c; \qquad (2)$$

this ultimately maximizes the axial-vector decay rate and thereby places the strongest bounds on our examples. Second, as a conservative benchmark, we assume that the heavier dark-matter particle χ_2 carries the vast majority of the dark-matter abundance, i.e., $\Omega_2 = 0.26$, $\Omega_1 = 0$. As we shall see, this assumption also maximizes the rates for all relevant processes and thereby places the strongest

bounds on our examples. Our main qualitative results ultimately will not depend on this choice; other choices such as $\Omega_1 \approx \Omega_2 \approx \Omega_{\text{CDM}}/2$ also lead to similar results.

Our examples thus have three parameters: c/Λ^2, m_2, and $\Delta m_{12} \equiv m_2 - m_1$. The $\Delta m_{12} \to 0$ limit embodies the physics of a traditional single-component dark sector with mass m_2. However, turning on Δm_{12} enables us to explore the effects of nonminimality in the dark sector. We restrict our attention to situations with $\Delta m_{12} \lesssim \mathcal{O}(\text{MeV})$, but there is no fundamental reason that larger Δm_{12} cannot also be considered. Note that a small mass splitting $\Delta m_{12} \ll m_1, m_2$ can be realized naturally in models wherein the generation of Δm_{12} is associated with the breaking of an approximate symmetry (see, e.g., Ref. [2]). Examples include models in which a Dirac fermion is split into a pair of nearly degenerate Majorana states by a small Majorana mass, and models in which a complex scalar is split into two real scalars by a small holomorphic mass.

We will now explore the resulting $(c/\Lambda^2, \Delta m_{12})$ parameter space for different values of m_2. Likewise, since we are taking $\Omega_1 = 0$ for simplicity, the relevant processes are limited to inelastic down-scattering, asymmetric collider production, and dark-matter decay.

Inelastic down-scattering.—We begin by considering the bounds from direct-detection experiments on the inelastic down-scattering process $\chi_2 N_i \to \chi_1 N_f$ where $N_{i,f}$ denote the initial and final states of the target nucleus N. For this, we use the nuclear form factors in Ref. [7]. Likewise, the corresponding bounds are derived using the most recent LUX [8] and COUPP-4 [9] data for the scalar and axial-vector interactions, respectively. Roughly speaking, this data can be taken as requiring $R \lesssim 1.81 \times 10^{-4}$ kg^{-1} day^{-1} and $R \lesssim 4.97 \times 10^{-2}$ kg^{-1} day^{-1} for the recoil-energy windows 3 keV $\leq E_R \leq 25$ keV and 7.8 keV $\leq E_R \leq 100$ keV, respectively.

While much of this analysis is completely standard, the primary new ingredient is the change in scattering kinematics from elastic to inelastic. The resulting recoil-energy range is shown in Fig. 2. This change in kinematics has two important consequences. First, we see that the required incoming velocity for down-scattering with $E_R \approx E_R^* \equiv [m_1/(m_1 + m_N)]\Delta m_{12}c^2$ is essentially zero. Indeed, the required input energy in this inelastic case comes directly from species conversion within the dark sector rather than from incoming dark-sector kinetic energy. Second, for any incoming dark-matter velocity v, we have both a finite *upper* limit as well as a nonzero *lower* limit on the allowed nuclear recoil energy E_R. In the case of down-scattering, this allowed range of recoil energies is centered around E_R^* and becomes exceedingly narrow as the incoming velocity goes to zero.

Asymmetric collider production.—Multicomponent operators such as those in Eq. (1) can also be probed through the collider production of dark matter. Because such production processes take the form $qq \to \chi_1\chi_2$, we are necessarily dealing with *asymmetric* (rather than symmetric) production. Nevertheless, these processes continue to be constrained through monojet searches at ATLAS [10] and CMS [11] as well as mono-W/Z searches at ATLAS [12]. These limits are directly applicable to the asymmetric production of χ_1 and χ_2 because Δm_{12} within our region of interest [i.e., $\Delta m_{12} \lesssim \mathcal{O}(\mathrm{MeV})$] is negligibly small compared to collider energy scales.

Dark-matter decay.—We now turn to an analysis of the new (diagonal) complementarity direction which comes into existence for nonzero Δm_{ij}, namely the possibility of decay from heavier to lighter dark-matter components.
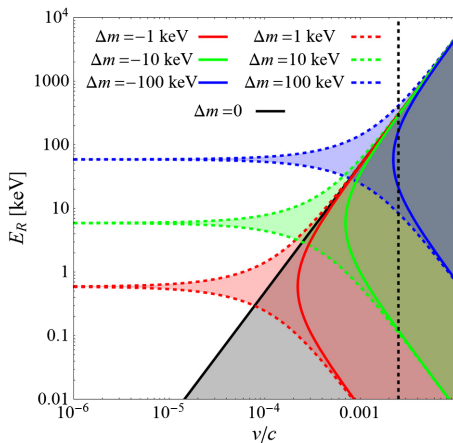

FIG. 2 (color online). Allowed ranges of recoil energy E_R as a function of incoming dark-matter particle velocity v for inelastic scattering $\chi_2 N_i \to \chi_1 N_f$ off a germanium nucleus, with $m_2 = 100$ GeV and different $\Delta m \equiv m_2 - m_1$. Results for both down-scattering ($\Delta m > 0$) and up-scattering ($\Delta m < 0$) are shown. Also shown is the elastic case (solid black line) as well as the maximum velocity cutoff associated with the galactic escape velocity (dashed black line).

Because we are considering dark-sector mass splittings of size $\Delta m_{12} \lesssim \mathcal{O}(\mathrm{MeV})$, dark-matter decay induced by the operators in Eq. (1) must be studied within the framework of chiral perturbation theory (ChPT) based on the low-energy $SU(2)_L \times SU(2)_R \times U(1)_V$ flavor symmetry group of the light (u, d) quarks. This allows us to generate a complete set of operators coupling dark matter to photons and pions, while capturing the symmetry structure of our underlying microscopic Lagrangian up to unknown (but ultimately measurable) coefficients $\tilde{\lambda}_i \sim \mathcal{O}(1)$. These operators turn out to take the form

$$\mathcal{L}_{\mathrm{eff}}^{(S)} = \frac{B_0 \alpha_{\mathrm{EM}} \tilde{\lambda}_2 c^{(S)}}{32\pi^3 f_\pi^2 \Lambda^2} (\bar{\chi}_2 \chi_1) F_{\mu\nu} F^{\mu\nu} + \cdots$$

$$\mathcal{L}_{\mathrm{eff}}^{(A)} = -\frac{2c^{(A)} f_\pi}{\Lambda^2} \left[1 + \frac{m_\pi^2}{16\pi^2 f_\pi^2} \tilde{\lambda}_3 \right] (\bar{\chi}_2 \gamma^\mu \gamma^5 \chi_1)(\partial_\mu \pi^0)$$

$$+ \frac{\alpha_{\mathrm{EM}} \tilde{\lambda}_4 c^{(A)}}{32\pi^3 f_\pi^2 \Lambda^2} (\bar{\chi}_2 \gamma^\mu \gamma^5 \chi_1) \partial_\mu (F_{\nu\rho} \tilde{F}^{\nu\rho}) + \cdots \quad (3)$$

where $B_0 \equiv m_\pi^2/(m_u + m_d)$ and $f_\pi \approx 93$ MeV.

As illustrated in Fig. 3, these interaction terms come in two types: contact operators which directly couple our dark-sector components χ_i to photons, and operators which couple our dark-sector components to off-shell pions (which then subsequently decay to two photons). These operators allow us to calculate the widths for the decays $\chi_2 \to \chi_1 \gamma\gamma$. For $\Delta m_{12} \ll m_{1,2}$, we obtain

$$\Gamma_{\gamma\gamma}^{(S)} \approx \tilde{\lambda}_2^2 \frac{B_0^2 \alpha_{\mathrm{EM}}^2 [c^{(S)}]^2 (\Delta m_{12})^7}{512(105\pi^9) f_\pi^4 \Lambda^4},$$

$$\Gamma_{\gamma\gamma}^{(A)} \approx \left[\tilde{\lambda}_3 - \tilde{\lambda}_4 + \frac{16\pi^2 f_\pi^2}{m_\pi^2} \right]^2 \frac{\alpha_{\mathrm{EM}}^2 [c^{(A)}]^2 (\Delta m_{12})^9}{512(315\pi^9) f_\pi^4 \Lambda^4}. \quad (4)$$

Note, in this context, that neither scalar or axial-vector interactions can lead to the process $\chi_2 \to \chi_1 \gamma$ via a charged-pion loop, because the photon can only couple to external fermion bilinears with a vector or tensor structure in a parity-invariant theory. By contrast, the process $\chi_2 \to \chi_1 \bar{\nu}\nu$ is possible, but will be suppressed by $\Delta m_{12}^4 G_F^2$; such processes are thus negligible, and will be ignored.

The decay rates in Eq. (4) may then be compared against existing bounds on observed photon fluxes: assuming an NFW profile for the dark-matter distribution [13], we use
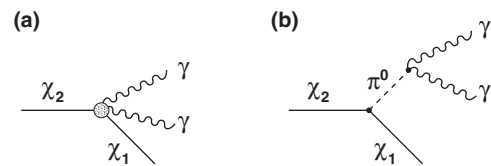

FIG. 3. Dominant dark-matter decay processes at energies $E \lesssim \mathcal{O}(10^2)$ keV, mediated by (a) an effective contact operator; or (b) off-shell neutral-pion exchange.

the PPPC4DMID software package [14] to determine the diffuse galactic and extragalactic contributions to the differential photon flux arising from dark-matter decay, and require that the predicted photon count not exceed that measured in any bin at the 2σ confidence level.

Results.—Combining the constraints from each of the dark-matter directions discussed above, we can now map out the current bounds on the operators in Eq. (1) in the $(c/\Lambda^2, \Delta m_{12})$ parameter space. Our results are shown in Fig. 4 for $m_2 = 100$ GeV, with $c^{(S)} = c^{(A)} = 1/\sqrt{2}$ and $\tilde{\lambda}_i = 1$ chosen as fixed reference values. The pink regions are excluded by bounds from the direct-detection experiments LUX (S) [8] and COUPP-4 (A) [9], while the green contour indicates the projected future reach of the LZ 7.2-ton detector (S) [15] and PICO-250L (A) [16]. Likewise, the vertical blue and cyan contours respectively correspond to LHC constraints on asymmetric collider production from monojet [10,11] and mono-W/Z [12] searches. The collider analysis was performed by generating signal events using the MADGRAPH 5 [17], PYTHIA 6.4 [18], and DELPHES 2.0.5 [19] software packages, and comparing to the number of background events reported in Refs. [10–12] in order to determine the region excluded at 90% C.L. There is a ~10% systematic uncertainty in the bounds on Λ. These collider-based bounds should be interpreted at best only heuristically if $\Lambda \lesssim \mathcal{O}(\text{TeV})$. The yellow and purple shaded regions are excluded by constraints on dark-matter decay from the total diffuse x-ray background measurements of HEAO-1 [20] and INTEGRAL [21], respectively. Finally, the diagonal dashed black lines from left to right respectively indicate contours corresponding to dark-matter lifetimes $\tau_2 = 10^{22}$ s, 10^{24} s, and 10^{26} s, while the solid black triangular regions in the upper left regions of each panel are excluded by requiring that $\tau_2 \gtrsim 4.35 \times 10^{17}$ s, the current age of the Universe. Note that mechanisms for having such long-lived dark-matter components can be found, for example, in Ref. [22].

There are many important features contained within Fig. 4. For $\Delta m_{12} \lesssim \mathcal{O}(10 \text{ keV})$, all of the features within these plots effectively reproduce the physics of a single-component dark sector with mass m_2. For $\Delta m_{12} \approx \mathcal{O}(10$–$100 \text{ keV})$, by contrast, the bounds from direct-detection experiments actually strengthen somewhat as a consequence of the kinematics of inelastic down-scattering, in some cases becoming comparable to monojet collider bounds for $\Delta m_{12} \approx \mathcal{O}(100 \text{ keV})$. Next, for $\Delta m_{12} \approx \mathcal{O}(100$–$1000 \text{ keV})$, one finds a "ceiling" for Δm_{12} beyond which direct-detection experiments cease to provide any bounds at all. Finally, for $\Delta m_{12} \gtrsim \mathcal{O}(\text{MeV})$, the dominant constraints now arise from dark-matter decay, with the maximum reach Λ_{max} scaling approximately as $(\Delta m_{12})^{7/4}$ and $(\Delta m_{12})^{9/4}$ for the scalar and axial-vector interactions, respectively.

The existence of the direct-detection "ceiling" is due to the unique kinematics associated with inelastic
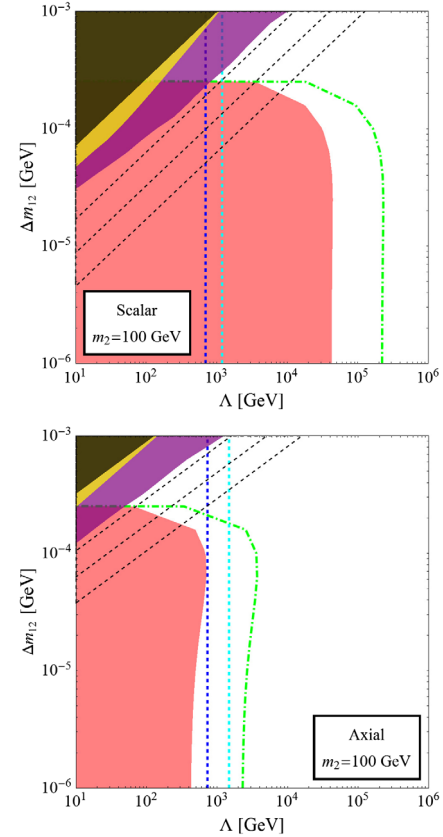

FIG. 4 (color online). Complementary bounds on the operators in Eq. (1), plotted as functions of Λ and Δm_{12} for $m_2 = 100$ GeV and $c^{(S)} = c^{(A)} = 1/\sqrt{2}$, as discussed in the text. Remarkably, we see that the constraints from dark-matter decay dominate in exactly those regions with relatively large Δm_{12} that lie beyond the reach of current and proposed direct-detection experiments, thereby illustrating the new sorts of complementarities that are possible for such multicomponent dark sectors.

down-scattering. For down-scattering there is a lower limit of nuclear recoil energies $E_R^{(\text{min})}$ below which the differential scattering rate dE_R/dR becomes negligible (see Fig. 2). However, for sufficiently large Δm_{12}, this minimum value begins to exceed the maximum recoil energy which current detectors can reliably probe. Indeed, a given dark-matter direct-detection experiment is typically designed to probe only a particular window of recoil energies. While the precise window of recoil energies depends on the type of experiment and the cuts imposed as part of the data analysis, this window typically falls within the range $1 \text{ keV} \lesssim E_R \lesssim 100 \text{ keV}$. Scattering events with recoil energies outside this range do not contribute to the measured signal-event rate. As a result, there exists a critical value of Δm_{12} beyond which the corresponding down-scattering events escape detection.

The plots in Fig. 4 provide dramatic illustration of the new complementarities that emerge within the context of nonminimal dark sectors. Together, these constraints not only increase the *coverage* of the corresponding parameter

space but also provide useful *correlations* between these processes in regions where these constraints overlap. For example, it is somewhat remarkable that the constraints from dark-matter decay emerge and dominate in exactly those regions that lie just beyond the Δm_{12} "ceiling" that caps the reach of current and proposed direct-detection experiments. This nontrivial structure is testament to the richness of the complementarities that emerge when Δm_{12} is lifted beyond the $\Delta m_{12} = 0$ axis to which the traditional complementarities of single-component dark sectors are effectively restricted.

Conclusions.—Complementarity has long infused our thinking about the hunt for dark matter, but most work has focused on the case of single-component dark sectors. In this Letter, we have considered a multicomponent dark sector and found that entirely new directions for complementarity open up. In particular, we studied correlations between *inelastic* scattering at direct-detection experiments, *asymmetric* dark-matter production at colliders, and indirect-detection signals due to dark-matter *decay*— the latter phenomenon having no analogue in the single-component context—and we demonstrated that these strategies can together provide complementary probes of the dark-sector parameter space. In particular, for large Δm_{12}, direct-detection experiments lose sensitivity precisely where the decay constraints dominate. This result is especially gratifying, given that any operators and initial conditions which give rise to inelastic down-scattering direct-detection signals in a multicomponent context must also necessarily give rise to dark-matter decays.

Needless to say, many future directions can be pursued [6]. For example, in addition to other operator structures, one can also consider nonminimal dark sectors with relatively large numbers of individual components [23], thereby potentially giving rise to collective effects that transcend the two-component effects studied here.

[1] S. Arrenberg *et al.*, arXiv:1310.8621.

[2] T. Han and R. Hempfling, Phys. Lett. B **415**, 161 (1997); L. J. Hall, T. Moroi, and H. Murayama, Phys. Lett. B **424**, 305 (1998); D. Smith and N. Weiner, Phys. Rev. D **64**, 043502 (2001); **72**, 063509 (2005); Y. Cui, D. E. Morrissey, D. Poland, and L. Randall, J. High Energy Phys. 05 (2009) 075.

[3] F. Chen, J. M. Cline, and A. R. Frey, Phys. Rev. D **79**, 063530 (2009); D. P. Finkbeiner, T. R. Slatyer, N. Weiner, and I. Yavin, J. Cosmol. Astropart. Phys. 09 (2009) 037; B. Batell, M. Pospelov, and A. Ritz, Phys. Rev. D **79**, 115019 (2009); P. W. Graham, R. Harnik, S. Rajendran, and P. Saraswat, Phys. Rev. D **82**, 063512 (2010).

[4] D. P. Finkbeiner and N. Weiner, Phys. Rev. D **76**, 083519 (2007); J. M. Cline, A. R. Frey, and F. Chen, Phys. Rev. D **83**, 083511 (2011); N. F. Bell, A. J. Galea, and R. R. Volkas, Phys. Rev. D **83**, 063504 (2011).

[5] M. Pospelov and A. Ritz, Phys. Rev. D **84**, 113001 (2011); A. Drozd, B. Grzadkowski, and J. Wudka, J. High Energy Phys. 04 (2012) 006; C. Cheung and Y. Nomura, Phys. Rev. D **86**, 015004 (2012); Y. Bai, P. Draper, and J. Shelton, J. High Energy Phys. 07 (2012) 192; S. Bhattacharya, A. Drozd, B. Grzadkowski, and J. Wudka, J. High Energy Phys. 10 (2013) 158; J. Wang, Phys. Rev. D **89**, 093019 (2014).

[6] K. R. Dienes, J. Kumar, B. Thomas, and D. Yaylali (to be published).

[7] N. Anand, A. L. Fitzpatrick, and W. C. Haxton, Phys. Rev. C **89**, 065501 (2014).

[8] D. S. Akerib *et al.* (LUX Collaboration), Phys. Rev. Lett. **112**, 091303 (2014).

[9] E. Behnke *et al.* (COUPP Collaboration), Phys. Rev. D **86**, 052001 (2012).

[10] G. Aad *et al.* (ATLAS Collaboration), J. High Energy Phys. 04 (2013) 075; ATLAS Collaboration, ATLAS-CONF-2012-147.

[11] S. Chatrchyan *et al.* (CMS Collaboration), J. High Energy Phys. 09 (2012) 094; CMS Collaboration, CMS-PAS-EXO-12-048.

[12] G. Aad *et al.* (ATLAS Collaboration), Phys. Rev. Lett. **112**, 041802 (2014); Phys. Rev. D **90**, 012004 (2014).

[13] J. F. Navarro, C. S. Frenk, and S. D. M. White, Astrophys. J. **462**, 563 (1996).

[14] M. Cirelli, G. Corcella, A. Hektor, G. Hütsi, M. Kadastik, P. Panci, M. Raidal, F. Sala, and A. Strumia, J. Cosmol. Astropart. Phys. 03 (2011) 051; 10 (2012) E01.

[15] R. Gaitskell *et al.*, http://dmtools.brown.edu:8080; D. C. Malling *et al.*, arXiv:1110.0103.

[16] R. Neilson, talk given at Aspen 2013, http://http://indico .cern.ch/event/197862/session/ 3/contribution/69/material/ slides/0.pdf.

[17] J. Alwall, M. Herquet, F. Maltoni, O. Mattelaer, and T. Stelzer, J. High Energy Phys. 06 (2011) 128.

[18] T. Sjostrand, S. Mrenna, and P. Z. Skands, J. High Energy Phys. 05 (2006) 026.

[19] S. Ovyn, X. Rouby, and V. Lemaitre, arXiv:0903.2225.

[20] D. E. Gruber, J. L. Matteson, L. E. Peterson, and G. V. Jung, Astrophys. J. **520**, 124 (1999).

[21] L. Bouchet, E. Jourdain, J. P. Roques, A. Strong, R. Diehl, F. Lebrun, and R. Terrier, Astrophys. J. **679**, 1315 (2008).

[22] M. Fairbairn and J. Zupan, J. Cosmol. Astropart. Phys. 07 (2009) 001; H. Fukuoka, J. Kubo, and D. Suematsu, Phys. Lett. B **678**, 401 (2009).

[23] K. R. Dienes and B. Thomas, Phys. Rev. D **85**, 083523 (2012); **85**, 083524 (2012).